Hybrid Additive Manufacturing of a Planar Dielectric Resonator Antenna Array at K-Band

Hehenberger, Simon P.; Caizzone, Stefano; Yarovoy, Alexander

DOI
10.23919/EuCAP63536.2025.10999635

Publication date
2025

Document Version
Final published version

Published in
Proceedings of the 2025 19th European Conference on Antennas and Propagation (EuCAP)

Hybrid Additive Manufacturing of a Planar Dielectric Resonator Antenna Array at K-Band

Simon P. Hehenberger*, Stefano Caizzone*, Alexander Yarovoy†,
*Institute of Communication and Navigation, German Aerospace Center, Oberpfaffenhofen, Germany, simon.hehenberger@dlr.de
†Microwave Sensing, Signals and Systems, TU Delft, Delt, The Netherlands

***Abstract*—The feasibility of using hybrid additive manufacturing (AM) to produce low-cost, phased array antennas for SatCom applications is investigated in this work. A 4x2 planar array comprised of dielectric resonator antennas (DRAs) operating in the fundamental mode within the K-band SatCom downlink band (17.7–21.2 GHz) has been designed, fabricated and measured. The impact of print settings on the material properties is assessed and incorporated into the antenna design process. Manufactured prototypes of the single element and the planar array geometry are experimentally verified in terms of their scattering parameters and far-field radiation patterns. The potential of combining hybrid AM and DRA technologies for future mmWave phased array developments is highlighted by the presented results.**

***Index Terms*—antennas, electromagnetics, propagation, measurements.**

I. Introduction

Modern mmWave phased array antennas face challenges in providing sufficient bandwidth at a cost suitable for mass-market applications. Over the past decade, additive manufacturing (AM) has gained traction in radio frequency (RF) and microwave applications, enabling complex geometries and rapid prototyping [1], [2]. AM has been successfully applied to produce both metallic and dielectric components, such as dielectric resonator antennas (DRA) with engineered permittivity [3], [4], graded index lenses [5], horn antennas [6], slotted waveguide antennas [7], and metallic lens designs [8] from a single material.

However, single-material AM processes are inherently limited, considering advanced designs requiring the combination of dielectric and conductive materials or interfacing with conventional microwave equipment. In the last few years, AM technology has matured sufficiently to combine dielectric and conductive materials within the same process. Techniques like inkjet printing of dielectric and conductive inks [9] and the combination of extrusion-type AM with micro-dispensing of conductive inks [10] are particularly promising. While inkjet printing offers exceptional accuracy, extrusion-based methods are more accessible and compatible with various materials.

Extrusion-based hybrid AM has been used to create various antenna designs and RF components [12] [13] [14]. However, most applications have been limited to sub-10GHz frequencies and essentially replicate designs that are already feasible with traditional methods. Regarding the utilization of AM for antenna applications, dielectric resonator antennas (DRAs) have emerged as a promising technology in the past decade, offering greater bandwidth and design flexibility for microwave and mmWave antennas compared to traditional microstrip patch antennas [15], [16] [17]. The combination of hybrid AM and DRAs holds significant potential for developing low-cost, high-performance mmWave phased array antennas. This is demonstrated in [18] through the full AM of an eight-element linear array of wideband multi-mode cylindrical DRAs with tailored dielectric properties. While [18], successfully showcases a wide range of AM capabilities the design does scale well to large scale planar arrays due the utilized sub-wavelength periodic structure manufactured from expensive high-permittivity material.

In this work we aim to minimize manufacturing complexity by utilizing a print material with moderate permittivity and a simplified DRA geometry. To this end, we present the design and full AM of a rectangular DRA element operating in its fundamental mode at the SatCom K-Band downlink band center frequency $f_c = 19.45$. Additionally, we demonstrate the antenna's performance in a 4×2 planar array configuration and its beam steering capabilities using a commercially available integrated circuit evaluation board. All presented prototypes are fully additive manufactured utilizing three different dielectrics and a conductive silver ink with a low-cost manufacturing setup.

The remainder of this work is structured as follows: Section II details the antenna's design and explains the print process's effect on the dielectric material parameters. Section III. explains the manufacturing setup and the utilized print parameters. Section IV. presents the measurement and simulation results of the antenna w.r.t. scattering parameters and far-field radiation. Furthermore, beam steering with an eight-channel integrated circuit is demonstrated. Finally, Section V. provides a conclusion to the presented work.

II. Design

A schematic drawing of the proposed antenna is depicted in Figure 1. The design process and individual steps are explained in detail below. The antenna is manufactured in two parts: the radiator with a mounting structure and the substrate incorporating the groundplane, feed aperture, and microstrip feed line. The DRA and its holding structure are printed

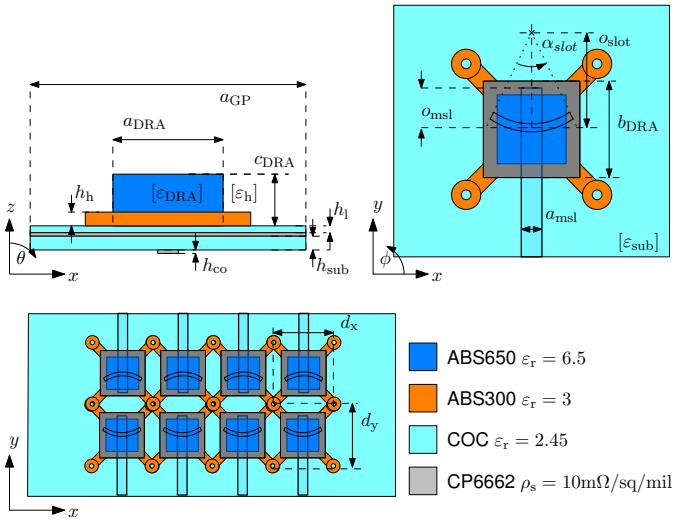

Fig. 1. Schematic drawing of the dielectric resonator antenna element considered in this work and its extension to an 2×4 array with color-coding corresponding to the different utilized materials in the additive manufacturing process.

using the thermoplastic dielectrics[1] ABS300 ($\varepsilon_{r,ABS300} = 3 \pm 0.1$; $\tan\delta_{ABS300} = 0.0046$) and ABS650 ($\varepsilon_{r,ABS650} = 6.5 \pm 0.15$; $\tan\delta_{ABS650} = 0.0034$) from Avient. The ground plane and feed microstrip are fabricated using the low-loss Cyclo-Olefin-Copolymer (COC) ($\varepsilon_{r,COC} = 2.45 \pm 0.1$; $\tan\delta_{COC} = 0.0004$) from Creamelt, and a highly conductive micro-dispensed silver ink (Bectron CP6662 from Elantas).

A. Single Element Design

The design of the single element is carried out in three steps.

(i) *Material Characterization:* Generally with AM, the final material parameters depend on the specific process settings utilized during the manufacturing. Therefore, a characterization of material properties is necessary to ensure an accurate design and predictable performance.

(ii) *DRA Dimension* An eigenmode solver is employed to determine the cuboid DRA dimensions ($a_{DRA} = b_{DRA}$ and c_{DRA}) that support the fundamental HEM_{111} mode at the desired antenna center frequency.

(iii) *Full-Wave Simulation:* Finally, an optimization within a full-wave simulation environment is carried out to find the dimensions α_{slot}, o_{slot}, and w_{slot} to produce a satisfying match of the antenna to the microstrip line.

Finally, the optimized single element is introduced into the 4×2 array geometry without further optimization.

1) Material Characterization: During manufacturing, the part is built up layer-by-layer through parallel lines of extruded thermoplastic. This process introduces tiny air gaps between the individual lines and layers. For the dielectric material properties, this implies, on the one hand, a reduced effective relative permittivity and, on the other hand, the introduction of a uni-axial anisotropic characteristic. [19] [20]. The anisotropic relative permittivity tensor of the materials concerning the utilized print settings, as reported in Section IV., as utilized in this work, are characterized via a waveguide setup as described in [20]. The effective relative permittivity tensors of the utilized dielectrics and print settings are

$$[\varepsilon_{r,ABS650}] = \begin{bmatrix} 6.05 & 0 & 0 \\ 0 & 6.04 & 0 \\ 0 & 0 & 5.08 \end{bmatrix} \quad (1)$$

$$[\varepsilon_{r,ABS300}] = \begin{bmatrix} 2.95 & 0 & 0 \\ 0 & 2.95 & 0 \\ 0 & 0 & 2.86 \end{bmatrix} \quad (2)$$

and,

$$[\varepsilon_{r,COC}] = \begin{bmatrix} 2.25 & 0 & 0 \\ 0 & 2.25 & 0 \\ 0 & 0 & 2.20 \end{bmatrix}. \quad (3)$$

Due to the low-loss nature of the individual dielectrics and the additional losses in the measurement system the characterization of the loss-tangent via this method is inaccurate. Therefore, the values for the materials loss tangents used in simulations are obtained from the respective datasheets as mentioned above, and the effect of print settings is not considered in this regard.

The Bectron CP 6662 silver ink requires thermal curing at a temperature of 120 °C for 10 minutes after dispensing. After the thermal curing the resistivity is measured with a four-point-probe system Jandel RM3-AR from Polytech GmbH to be about $\rho_s = 12$ mΩ/sq for a layer height of 40µm, corresponding well to the value reported in the datasheet of the ink (10 mΩ/sq/mil).

2) DRA dimensions: Generally, the resonance frequencies for individual modes in a rectangular DRA can be easily found via the dielectric waveguide model, as reported in [21]. However, these analytical tools are rendered inaccurate for use in this work due to the non-regular shape and multi-material composition of the DRA. Therefore, a numerical solver to compute the antenna modes is employed to identify suitable DRA dimensions, supporting the desired mode at the desired antenna center frequency. For this purpose the DRA, as depicted in Figure 1 is modeled in the CST eigenmode solver environment with dielectric material properties according to the characterization results reported in equations (2) and (1) and holding structure dimensions $h_h = 0.75\text{mm}$ and $w_h = 0.75\text{mm}$. For DRA dimensions $a_{DRA} = b_{DRA} = 5.24$, mm and $c_{DRA} = 2.55$ mm the desired mode exhibits a resonance frequency of 19.6 GHz and a quality factor $Q = 4$;

3) Element feed: The antenna is excited using a 50Ω microstrip transmission line on a substrate with height h_{sub}. The antenna and transmission line are coupled via an arc-shaped slot centrally below the dielectric resonator characterized via the geometric parameters o_{slot}, α_{slot} and w_{slot}. The transmission line is terminated with an open at an offset of o_{msl} w.r.t. the center of the DRA. The DRA is mounted on the substrate via four countersunk M2 nylon screws. Since

[1]datasheets available upon request from the manufacturer

TABLE I
GEOMETRIC PARAMETERS OF PROPOSED DIELECTRIC RESONATOR ANTENNA DESIGN.

Variable	Value	Variable	Value
$a_{\text{DRA}} = b_{\text{DRA}}$	5.24 mm	c_{DRA}	2.55 mm
a_{GP}	50 mm	h_{sub}	0.48 mm
w_{h}	0.75 mm	h_{h}	0.75 mm
a_{msl}	1.5 mm	o_{msl}	3.5 mm
o_{slot}	2.75 mm	α_{slot}	114°
h_{l}	0.24 mm	h_{co}	40 µm

printing conductive ink directly to the heated print bed is not possible, an additional layer of substrate with height h_{l}, further referred to as spacer, between the ground plane and the DRA, is considered in the design. For later manufacturing, a layer height of 0.12mm is selected for the feed substrate. It is desired to extrude two and four layers for the spacer substrate and microstrip substrate, respectively, resulting in $h_{\text{l}} = 0.24\text{mm}$ and $h_{\text{sub}} = 0.48\text{mm}$. The microstrip substrate exhibits a permittivity of $\varepsilon_{\text{r,sub}} = \varepsilon_{\text{r,COC}}$, as reported in (3) above, and the conductive ink is dispensed with 0.04mm layer height, which implies a line width of $a_{\text{msl}} = 1.5\text{mm}$ to realize a characteristic impedance of $Z_0 = 50\Omega$. The remaining parameters of the feed structure, namely the dimensions of the coupling aperture o_{slot}, α_{slot}, as well as the microstrip termination offset o_{msl}, are subject to an optimization routine in a full-wave simulation environment to minimize the input reflection coefficient at the resonance frequency obtained from the eigenmode simulation as explained above. All geometric parameters are summarized in Table I.

B. Array

The designed element, without further optimization, is introduced into the 2×4 array geometry with a half-wavelength spacing at f_{c} corresponding to an inter-element distance $d_{\text{x}} = d_{\text{y}} = 7.7\text{mm}$, as indicated in Figure 1. The arm-length of the holding structure is chosen so that the mounting holes of neighboring elements coincide.

III. MANUFACTURING

A. Hardware Setup and Print Parameters

The manufacturing setup is based on a *core-XY* tool-changing concept based on the E3D motion system platform equipped with four independent tools that can be switched during the print process, allowing for flexible multi-material printing. In our case, the system is equipped with three E3D Hemera filament extruders for the three utilized dielectrics and a third-party printhead, Vipro-HEAD 3 from VisoTec GmbH, for silver ink dispensing. The ViproHead printhead is selected due to its precise dispensing capabilities and stepper motor interface, which allows straightforward integration into the existing print hardware. The hardware setup is summarized in Table II, and the corresponding print settings are reported in Table III.

TABLE II
HARDWARE CONFIGURATION OF THE TOOLCHANGER ADDITIVE MANUFACTURING SETUP.

E3D Motion System - Toolchanger Configuration				
Tool	**1**	**2**	**3**	**4**
Device	E3D Hemera Extruder	E3D Hemera Extruder	ViscoTec vipro-HEAD 3	E3D Hemera Extruder
Material	Avient ABS1500	Avient ABS300	Elantas Bectron CP6662	Creamelt COC
Orifice diameter	0.15mm	0.15mm	0.2mm	0.6mm

TABLE III
MATERIAL PRINT SETTINGS

Setting - Material	**ABS650**	**ABS300**	**CP6662**	**COC**
Extrusion width [mm]	0.15	0.15	0.2	0.6
Nozzle temp. [°C]	245	230	-	245
Bed temp. [°C]	105	105	55	75
Max. speed [mm s^{-1}]	5	7.5	7.5	60
Max. acc. [mm s^{-2}]	200	200	100	1500
Layer height [mm]	0.12	0.12	0.04	0.12

B. RF interface

In order to support measurements of the manufactured antennas, an interface from the microstrip feed network to the measurement equipment needs to be established. In this work, we utilize a 2.92mm SMA connector (Amphenol SF1521-60061) that is screwed onto the substrate and establishes a reliable connection via compression. The choice of the connector is driven by the necessity to employ a low-temperature solution because the utilized substrate material has a comparably low glass-transition temperature of $80°\text{C}$, which renders it incompatible with soldering techniques.

The manufactured array prototypes are depicted from the front and back in Figure 2

IV. SIMULATION AND MEASUREMENT

Both the single-element antenna as well as the 4×2 array geometry are characterized in terms of their scattering parameters and far-field radiation. Far-field measurements are carried out via a benchtop anechoic chamber solution from Millibox. The mounting of the manufactured array prototype together with the beamforming board on the measurement chamber positioner is depicted in Figure 3.

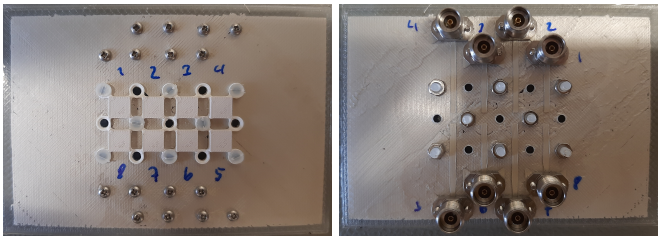

(a) (b)

Fig. 2. Manufactured prototype of the 4×2 array geometry (a) front, (b) back.

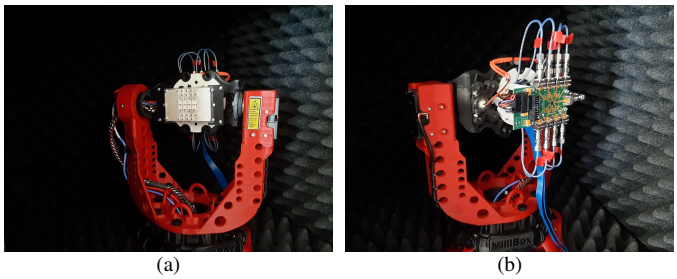

(a) (b)

Fig. 3. Array prototype, connected to the Anokiwave AWMF-0197 beamforming board, mounted on the positioner of the Millibox benchtop anechoic chamber.

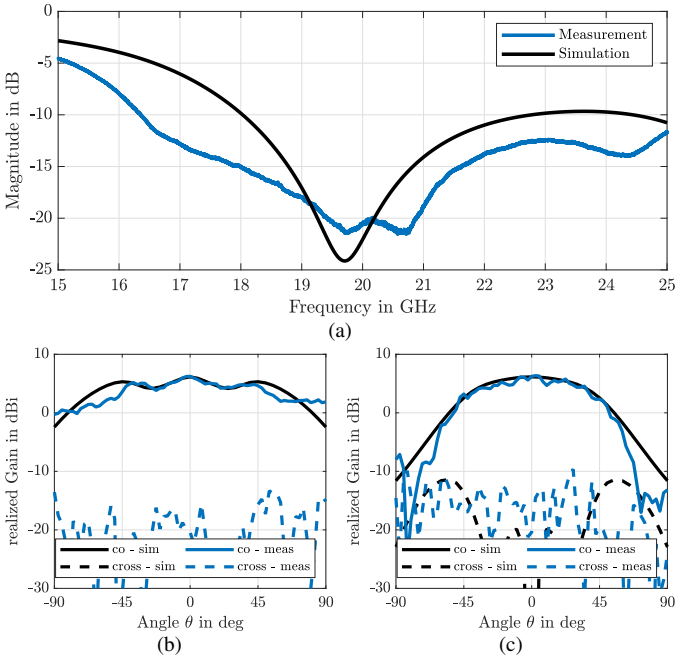

Fig. 4. Measurement results of the single element antenna prototype compared to simulation results. (a) Input reflection coefficient as a function of frequency. (b),(c) Co- and cross-polarized realized gain values at 19.4 GHz for $\phi = 0°$ and $\phi = 90°$.

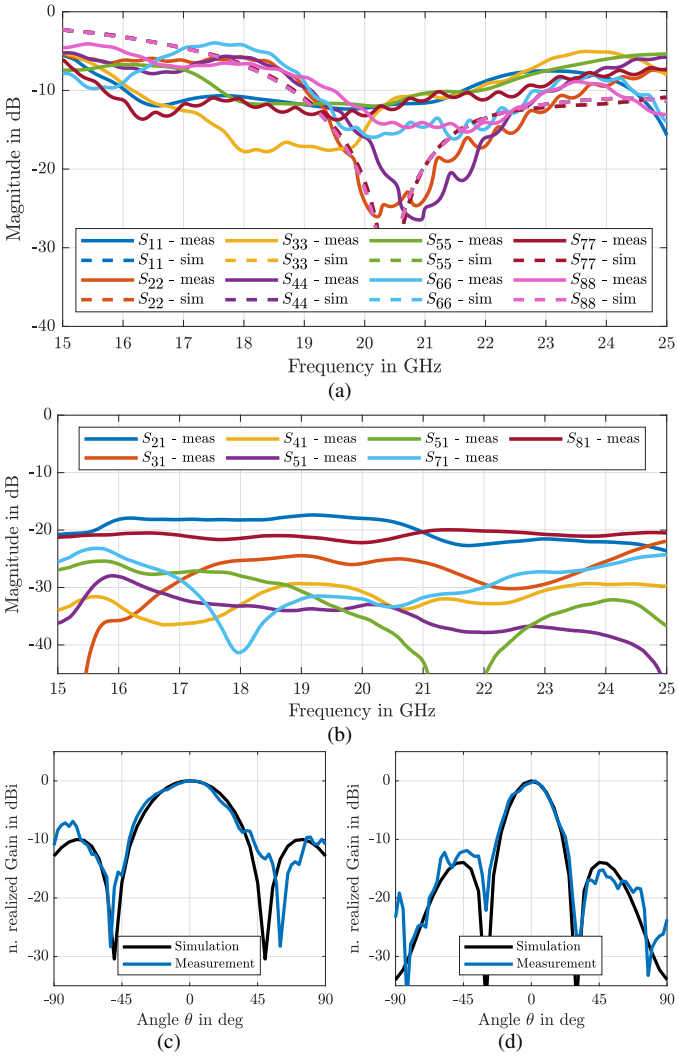

Fig. 5. Measurement results of the phased array antenna prototype compared to simulation results. Scattering parameters of the passive array, (a) self and (b) mutual terms, as a function of frequency. (c),(d) Co- and cross-polarized realized gain values at 19.4 GHz for $\phi = 0°$ and $\phi = 90°$.

A. Single Element

The single DRA element is characterized regarding input reflection coefficient and far-field radiation. The measured input reflection coefficient and results obtained through full-wave simulations are compared in Figure 4a. Furthermore, the measured co- and cross-polarized realized gain patterns are displayed for orthogonal azimuth cuts at the center frequency in Figure 4b and 4c. The impedance of the manufactured antenna compares well to the simulated values and is well matched at the intended design frequency of $f_c = 19.4$GHz. The presented realized gain measurements agree well with the simulated patterns; some discrepancies can be observed only for higher angles of the angle θ.

B. Array

The embedded elements of the 4×2 planar array with $\lambda/2$ spacing at the center frequency f_c are first characterized in terms of their input impedance and coupling and then connected to the evaluation board of the Anokiwave AWMF-0197, a commercially available integrated circuit intended for satellite communication receivers operating in the desired frequency range. The results of the impedance characterization measurements are depicted in Figure 5a and 5b respectively. The measured combined normalized realized gain, after a simple calibration of the individual amplitude and phase weights of the individual channels at 19.4GHz, is compared in Figures 5c and 5d respectively. The embedded elements are well matched for frequencies between 19.2GHz and 21.6GHz with coupling to neighboring elements not exceeding -17.5dB within this frequency range. The combined beampattern measurement corresponds well with what is predicted by the full-wave simulation. The combined pattern is presented in a normalized manner due to the coherent gain of the beamforming chip that was not considered in the simulation.

V. Conclusion

This study demonstrates the feasibility of realizing planar K-band arrays for SatCom applications using low-cost additive manufacturing (AM) techniques. We designed and fabricated a simple dielectric resonator phased array antenna using multi-material extrusion-based additive techniques combined with micro-dispensing of highly conductive silver particulate ink. The DRA design incorporates two different dielectric thermoplastic materials, one with moderate relative permittivity for the core of the resonator and the second with low relative permittivity to co-print a holding structure, providing easy placement and mounting of the array on the feed substrate. A low-loss dielectric material, along with dispensed silver ink, is used to create a planar network to excite the individual antenna elements via an aperture-coupled microstrip line. The entire manufacturing process is carried out using a low-cost system based on off-the-shelf components.

A necessary step in the design of antennas for manufacturing with AM is the characterization of dielectric and conductive material properties and their dependence on the process parameters. The design presented in this work incorporates the effect of print settings on the material parameters of the utilized dielectrics and conductive ink.

The manufactured antenna is validated through impedance and far-field measurements in both standalone and embedded configurations. Additionally, beamforming is demonstrated using a dedicated integrated circuit and a simple calibration procedure. Despite some remaining manufacturing imperfections, the measured array parameters closely match the simulated ones.

While hybrid manufacturing technology still requires advancements to reliably produce K-band components, this work highlights the substantial potential of low-cost hybrid additive techniques for mmWave applications. The results of this study suggest a promising future for these technologies in the development of advanced antenna systems for mmWave frequency bands where lightweight, customizable, and high-performance solutions are increasingly demanded.

VI. Acknowledgement

The authors acknowledge the efforts of and are thankful to Ms. Aparna P. T. Adithyababu for her support in performing the antenna measurement.

References

[1] E. S. Rosker, R. Sandhu, J. Hester, M. S. Goorsky, and J. Tice, 'Printable materials for the realization of high performance RF components: Challenges and opportunities', Int. J. Antennas Propag., vol. 2018, pp. 1–19, 2018.

[2] T. Whittaker, S. Zhang, A. Powell, C. J. Stevens, J. Y. C. Vardaxoglou, and W. Whittow, '3D Printing Materials and Techniques for Antennas and Metamaterials: A survey of the latest advances', IEEE Antennas Propag. Mag., vol. 65, no. 3, pp. 10–20, Jun. 2023.

[3] Q. Lamotte et al., 'Multi-permittivity 3D-printed ceramic dual-band circularly polarized dielectric resonator antenna for space applications', in 2021 15th European Conference on Antennas and Propagation (EuCAP), Dusseldorf, Germany, 2021.

[4] S. P. Hehenberger, S. Caizzone, and A. G. Yarovoy, 'Additive manufacturing of linear continuous permittivity profiles and their application to cylindrical dielectric resonator antennas', IEEE Open J. Antennas Propag., vol. 4, pp. 373–382, 2023.

[5] J. W. Allen and B.-I. Wu, 'Design and fabrication of an RF GRIN lens using 3D printing technology', in Terahertz, RF, Millimeter, and Submillimeter-Wave Technology and Applications VI, San Francisco, California, USA, 2013.

[6] A. Sharma, R. K. Stilwell, S. Szczesniak, and C. Carpenter, '3D metal printed Ka-band quad-ridge horn antenna', in 2022 IEEE International Symposium on Antennas and Propagation and USNC-URSI Radio Science Meeting (AP-S/URSI), Denver, CO, USA, 2022.

[7] T. Van Trinh, J. Park, C. M. Song, S. Song, and K. C. Hwang, 'A 3-D metal-printed dual-polarized ridged waveguide slot array antenna for X-band applications', Appl. Sci. (Basel), vol. 13, no. 8, p. 4996, Apr. 2023.

[8] D. Shamvedi, P. O'Leary, and R. Raghavendra, 'Development of 3D printed metallic lenses', in 2023 17th European Conference on Antennas and Propagation (EuCAP), Florence, Italy, 2023.

[9] X. Yu et al., "3-D Printed Parts for a Multilayer Phased Array Antenna System," in IEEE Antennas and Wireless Propagation Letters, vol. 17, no. 11, pp. 2150-2154, Nov. 2018.

[10] M. Li, Y. Yang, F. Iacopi, J. Nulman and S. Chappel-Ram, "3D-Printed Low-Profile Single-Substrate Multi-Metal Layer Antennas and Array With Bandwidth Enhancement," in IEEE Access, vol. 8, pp. 217370-217379, 2020.

[11] B.Niese, P. Amend, T. Frick, S. Roth and M. Schmidt, "Fast and flexible production of mechatronic integrated devices by means of additive manufacturing," 2016 12th International Congress Molded Interconnect Devices (MID), Wuerzburg, Germany, 2016.

[12] S. P. Hehenberger, S. Caizzone and A. Yarovoy, "Low-Cost Hybrid Additive Manufacturing of a Miniaturized Dual Band Stacked Patch Antenna for GNSS Applications," 2024 18th European Conference on Antennas and Propagation (EuCAP), Glasgow, United Kingdom, 2024.

[13] K. H. Church et al., "Multimaterial and Multilayer Direct Digital Manufacturing of 3-D Structural Microwave Electronics," in Proceedings of the IEEE, vol. 105, no. 4, pp. 688-701, April 2017.

[14] T. P. Ketterl et al., "A 2.45 GHz Phased Array Antenna Unit Cell Fabricated Using 3-D Multi-Layer Direct Digital Manufacturing," in IEEE Transactions on Microwave Theory and Techniques, vol. 63, no. 12, pp. 4382-4394, Dec. 2015

[15] S. Keyrouz and D. Caratelli, "Dielectric Resonator Antennas: Basic Concepts, Design Guidelines, and Recent Developments at Millimeter-Wave Frequencies," International Journal of Antennas and Propagation, vol. 2016. Hindawi Limited, pp. 1–20, 2016.

[16] F. P. Chietera, R. Colella, and L. Catarinucci, "Dielectric Resonators Antennas Potential Unleashed by 3D Printing Technology: A Practical Application in the IoT Framework," Electronics, vol. 11, no. 1. MDPI AG, p. 64, Dec. 26, 2021.

[17] N. A. Abd Rahman et al., "A Review of Circularly Polarized Dielectric Resonator Antennas: Recent Developments and Applications," Micromachines, vol. 13, no. 12. MDPI AG, p. 2178, Dec. 08, 2022.

[18] S. P. Hehenberger, S. Caizzone, A. Yarovoy, "Hybrid Additive Manufacturing of a Dielectric Resonator Phased Array Antenna at K-Band", Presented at, and to be published in the proceedings of the IEEE Phased Array Symposium 2024 (available on request)

[19] A. Goulas et al., "The impact of 3D printing process parameters on the dielectric properties of high permittivity composites," Designs, vol. 3, no. 4, p. 50, Nov. 2019

[20] S. P. Hehenberger, S. Caizzone, and A. Yarovoy, "Modeling and measurement of dielectric anisotropy in materials manufactured via fused filament fabrication processes," Materials Research Bulletin, vol. 179. Elsevier BV, p. 112938, Nov. 2024.

[21] R. Kumar Mongia and A. Ittipiboon, "Theoretical and experimental investigations on rectangular dielectric resonator antennas," IEEE Transactions on Antennas and Propagation, vol. 45, no. 9. Institute of Electrical and Electronics Engineers (IEEE), pp. 1348–1356, 1997.